Published as: *Geobiology*. 2012 May ; 10(3): 216–222.

Photomixotrophic growth of *Rhodobacter capsulatus* SB1003 on ferrous iron

Sebastian H. Kopf[1] and **Dianne K. Newman**[1,2,3]

Dianne K. Newman: dkn@caltech.edu

[1]Division of Geological and Planetary Sciences, Pasadena, CA 91125

[2]Division of Biological Sciences, California Institute of Technology, Pasadena, CA 91125

[3]Howard Hughes Medical Institute, Pasadena, CA 91125

Abstract

This study investigates the role iron oxidation plays in the purple nonsulfur bacterium *Rhodobacter capsulatus* SB1003. This organism is unable to grow photoautotrophically on unchelated ferrous iron [Fe(II)] despite its ability to oxidize chelated Fe(II). This apparent paradox was partly resolved by the discovery that SB1003 can grow photoheterotrophical-ly on the photochemical breakdown products of certain ferric iron - ligand complexes, yet whether it could concomitantly benefit from the oxidation of Fe(II) to fix CO_2 was unknown. Here, we examine carbon fixation by stable isotope labeling of the inorganic carbon pool in cultures growing phototrophically on acetate with and without Fe(II). We show that *R. capsulatus* SB1003, an organism formally thought incapable of phototrophic growth on Fe(II), can actually harness the reducing power of this substrate and grow photomixtotrophically, deriving carbon both from organic sources and fixation of inorganic carbon. This suggests the possibility of a wider occurrence of photoferrotrophy than previously assumed.

1. Introduction

Microbial processes throughout Earth's history have had a profound impact on the biogeochemical cycling of iron (Kappler and Straub, 2005; Ehrlich and Newman, 2008). While much attention has been paid to iron's ability to serve as an electron donor or electron acceptor in catabolic processes, beyond a crude accounting for electrons in the metabolisms of a few model organisms, we have little appreciation for how cells make use of iron's redox chemistry. For example, we would expect multiple elements within a cell to be affected by an imbalance in iron homeostasis, which in turn would be expected to change how a cell might regulate its export or uptake of substrates containing these elements. Similarly, we would expect intracellular redox homeostasis to be influenced by iron in myriad ways. How these and other more subtle effects manifest themselves is poorly understood, yet they may be important drivers of the overall iron biogeochemical cycle.

Correspondence to: Dianne K. Newman, dkn@caltech.edu.

In recognition of this knowledge gap, we chose to explore how ferrous iron [Fe(II)] is used by the anoxygenic phototroph, *Rhodobacter capsulatus* strain SB1003. We chose this organism as a model system because it exhibited a curious phenotype during phototrophic growth. Unlike other *Rhodobacter* species (Ehrenreich and Widdel, 1994), *R. capsulatus* SB1003 does not oxidize iron (and grow photolithotrophically) in medium containing Fe(II) chloride as the sole source of reducing power (Croal et al., 2007). However, in the presence of chelating agents such as citrate and NTA, Fe(II) oxidation is enabled and SB1003 can grow photoheterotrophically on supplementary carbon sources (Croal et al., 2007; Poulain and Newman, 2009), or, in the case of photoactive ferric [Fe(III)]-ligand complexes such as Fe(III)-citrate, on the photochemical breakdown products of the ligand (Caiazza et al., 2007). This shows that Fe(II) oxidation can benefit the organism indirectly but does not resolve whether Fe(II) oxidation can benefit *R. capsulatus* directly. (Poulain and Newman, 2009) first explored the ambiguous role of Fe(II) oxidation in *R. capsulatus* SB1003 and proposed Fe(II) oxidation as a potential detoxification mechanism. Preliminary data on gene expression furthermore revealed that several Calvin cycle genes are upregulated in the presence of Fe(II) (Poulain and Newman, unpublished data), suggesting a potential link to Fe(II) oxidation. Herein, we expand on these studies and show that *R. capsulatus* SB1003 can grow photomixotrophically using Fe(II) as an electron donor for carbon fixation.

2. Results and Discussion

2.1 Fe(II) oxidation promotes growth

To elucidate whether Fe(II) oxidation itself confers any growth benefit to *R. capsulatus*, we assessed phototrophic growth on Fe(II) complexed by nitrilotriacetate (NTA) in anoxic freshwater medium, completely devoid of additional electron donors (trace organics or hydrogen, see Materials and Methods), with bicarbonate as the sole carbon source (Figure 1). The lack of growth in the control experiment (NTA only) shows that *R. capsulatus* cannot use NTA as a carbon source. When provided with Fe(II)-NTA in the light, the organism grew rapidly for 2 days and appeared to grow slowly for the remainder of the experiment. Optical density likely reflects growth as iron oxides did not precipitate (all Fe(III) complexed by NTA), although small variations in optical density could also be due to morphological changes as the cells aged. Fe(II) was completely oxidized after 2 days (data not shown) and remained oxidized for the remainder of the experiment. No growth or Fe(II) oxidation occurred in the dark (Figure 1). When provided with Fe(III)-NTA instead, the organism had no direct source of reducing power and showed only very little growth, similar to later stage (2+ days) on Fe(II)-NTA (Figure 1). Small quantities of reduced Fe(II) (360±80 μM) accumulated in the medium within 2 days. Since the Fe(III)-NTA complex can be photochemically active at the experimental pH and light regime (Andrianirinaharivelo et al., 1993), the observed accumulation of Fe(II) is likely due to photoreduction of Fe(III) in the Fe(III)-NTA complex. This process is expected to photodegrade the ligand, yielding NTA breakdown products that could serve as a carbon source for photoheterotrophic growth ordissimilatory Fe(III) reduction (Dobbin et al., 1996). The apparent slow growth in the presence of Fe(III)-NTA, both when supplied initially or provided by oxidation of Fe(II), suggests that the organism can benefit from photoreduction of Fe(III), photolytic breakdown of NTA, or both. Because Fe(II)-NTA does not photolyze, and photolysis of unbound NTA

is exceedingly slow (Larson and Stabler, 1978), the rapid initial growth in the presence of Fe(II)-NTA cannot be explained by growth on photochemical breakdown products and suggests that the oxidation of Fe(II) provides a growth benefit to *R. capsulatus*.

2.2 Fe(II) oxidation allows for carbon fixation

To test whether Fe(II) serves as an electron donor for carbon fixation, we conducted isotope labeling experiments with ^{13}C labeled bicarbonate. If CO_2 is fixed during growth on Fe(II)-NTA, inorganic ^{13}C should be strongly incorporated into cell carbon. However, purple non-sulfur bacteria like *R. capsulatus* also use CO_2 as a sink for excess reducing equivalents to achieve redox homeostasis during photoheterotrophic growth (Tabita, 2004), potentially obscuring this signal. This is further complicated by any potential contribution to growth from photolytic breakdown products of NTA, which would introduce unlabeled carbon into the cell. To allow a quantitative interpretation of the labeling experiments, we thus explored three different growth conditions: phototrophic growth on [A] acetate alone, [B] Fe(II)-NTA alone, and [C] acetate and Fe(II)-NTA together. Table 1 documents optical density as well as acetate and Fe(II) concentrations at the onset and conclusion of each experiment, in addition to the^{13}C content of the harvested cells (see Materials and Methods for experimental details). Because all organic carbon sources were unlabeled (acetate, NTA) and the entire inorganic pool was labeled (bicarbonate), these isotopic data represent the net assimilation of organic vs. inorganic carbon into biomass for each growth condition. The low variability between biological replicates provides confidence in the reproducibility and comparability of the experimental conditions.

The isotopic data from growth condition [A] (acetate only) illustrates the role of carbon fixation for redox homeostasis during photoheterotrophic growth. During photoheterotrophic growth, purple non-sulfur bacteria like *R. capsulatus* generate energy from cyclic phosphorylation while building cell carbon directly from organic carbon sources. The use of organic substrates for biosynthesis, however, can lead to a buildup of excess reducing power, requiring these phototrophs to find an electron sink to maintain redox homeostasis. In organisms limited fornitrogen, nitrogenase can serve this function by sinking excess electrons into N_2 and H^+, producing ammonium and H_2(Hillmer and Gest, 1977; Mckinlay and Harwood, 2011). Additionally, certain alternative electron acceptors such as dimethylsulfoxide can provide the necessary electron sink (Richardson et al., 1988). More commonly though, redox homeostasis under photoheterotrophic growth of *R. capsulatus* is achieved by using CO_2 as a sink for excess reducing equivalents through the Calvin-Benson-Bassham pathway (the Calvin cycle) (Tichi and Tabita, 2000, 2001; Bauer et al., 2003; Tabita, 2004). During the experimental conditions employed in this study, photoheterotrophic growth of *R. capsulatus* in the presence of excess ammonium and the absence of alternative electron acceptors, CO_2 fixation via the Calvin cycle provides the only available sink for excess reducing power. This introduces cell carbon derived from the inorganic carbon pool into the cell. Our data indicate that close to 17% (Table 1) of cellular carbon is derived from the inorganic carbon poolduring photoheterotrophic growth of *R. capsulatus* SB1003 on acetate. This result is in agreement with a detailed metabolic flux analysis of another purple phototroph, *Rhodopseudomonas palustris*, growing photoheterotrophically on acetate (Mckinlay and Harwood, 2010): *R. palustris* metabolizes

22% of the provided acetate to CO_2 via central metabolic pathways and reincorporates 68% of the released CO_2 into cell carbon via the Calvin cycle, ultimately deriving approximately 16% of its cellular carbon from CO_2(Mckinlay and Harwood, 2010). Several pathways of acetate assimilation that can explain the observed exchange of carbon with the inorganic pool have been discovered in the purple phototrophs (Blasco et al., 1989; Willison, 1998; Filatova et al., 2005; Meister et al., 2005). However, why these organisms build up excess reducing power (that is disposed of via the Calvin cycle or other redox sinks) during growth on substrates that are more oxidized than cell carbon is still poorly understood (Mckinlay and Harwood, 2010). Under the experimental conditions employed in this study, the energetic cost of carbon fixation via the Calvin cycle is unlikely to significantly affect the energy available to *R. capsulatus*. ATP generation via cyclic photophosphorylation provides energy independently of the growth-limiting sources of reducing power (organic carbon and Fe(II)).

The large incorporation of labeled inorganic carbon in cultures grown phototrophically on Fe(II)-NTA alone (close to 63%, growth condition [B], see Table 1) confirms that Fe(II) serves as an electron donor for carbon fixation. However, the dilution of the inorganic signal (99% ^{13}C) indicates that *R. capsulatus* must be capable of assimilating some organic carbon from the chelator NTA, the only unlabeled pool of carbon available in the medium. Because the organism is unable to metabolize NTA directly (Figure 1), the isotopic data suggest that it can benefit from photolysis of the ligand. Previous studies (Caiazza et al., 2007) have shown that under similar conditions, growth of *R. capsulatus* SB1003 on Fe(II)-citrate occurs as a result of Fe(II) oxidation and Fe(III)-citrate photochemistry, which produces acetoacetic acid as a consequence of ligand breakdown, a carbon source accessible to the organism. A similar model is conceivable for Fe(II)-NTA with the well studied photochemically active Fe(III)-NTA complex breaking down to iminodiacetic acid (IDA), formaldehyde (HCHO), CO_2 and hydroxyl radicals (Trott et al., 1972; Stolzberg and Hume, 1975; Andrianirinaharivelo et al., 1993; Bunescu et al., 2008). IDA can further disintegrate to formaldehyde and glycine, although this second photolytic step proceeds at slower rates (Stolzberg and Hume, 1975). Based on the presence of genes annotated as hydroxymethyl-transferase (*glyA*, RCC00438), serine-glyoxylate aminotransferase (RCC03109) and hydroxypyruvate reductase (*ttuD*, RCC02615) in the sequenced genome of *R. capsulatus* SB1003, formaldehyde assimilation by the serine pathway shouldbe possible in SB1003, making for maldehydea potential carbon source(Chistoserdova et al., 2003). This pathway is a common functional module in methylotrophs and well understood at the biochemical level. An additional pathway of formaldehyde metabolism using the glutathione-dependent formaldehyde dehydrogenase (*adhC*, RCC00869) present in the genome of SB1003 is also possible as pointed out previously (Caiazza et al., 2007). This pathway leads to the net generation of reducing equivalents by oxidizing formaldehyde and could be used for fixing inorganic carbon but would not lead to direct assimilation of the organic carbon (which is oxidized to CO_2). *R. capsulatus* is unable to grow photoheterotrophically on IDA (no growth observed on 5mM IDA over the course of 3 days, data not shown) but can grow on glycine as the sole carbon source (growth on 5mM glycine up to an optical density of 0.3 at 675nm, data not shown), rendering glycine an additional potential source for carbon. Lastly, the radicals formed during Fe(III)-NTA photolysis can potentially interact with NTA or IDA

to provide additional accessible, yet unidentified carbon sources. Our isotopic data provides evidence that *R. capsulatus* can assimilate some of these NTA breakdown products, however, which photolytic product of NTA degradation is metabolized by the organism and how, remains to be shown.

The intermediate incorporation of labeled inorganic carbon in cultures grown phototrophically on acetate and Fe(II)-NTA (28%, growth condition [C], see Table 1) is consistent with a combination of the effects observed during growth on acetate alone and growth on Fe(II)-NTA alone (conditions [A] and [B]).

These results indicate that *R. capsulatus* SB1003 grows photomixotrophically by fixing CO_2 with Fe(II) as the electron donor (photoautotrophic metabolism) while simultaneously assimilating organic carbon sources (photoheterotrophic metabolism). Why the organism can benefit from the oxidation of Fe(II)-NTA but fails to oxidize unchelated $Fe^{2+}$is unclearand merits further research. It could reflect a requirement for ligand-bound Fe(II) to be recognized for efficient uptake into the cell, and/or result from a toxic effect of the free metal ion, as suggested by (Poulain and Newman, 2009).

2.3 Mass balance model

The isotopic data shows that *R. capsulatus* can incorporate a mixture of carbon sources during phototrophic growth and provides a basis for quantitative evaluation of their respective contributions. In the presence of complexed Fe(II), the organism seems capable of exploiting simple, naturally wide-spread organic acids (such as acetate), photochemically mobilized refractory carbon (such as ligand breakdown products) as well as the reducing power of the Fe(II) itself (summarized schematically in Figure 2). Isotopic mass balance yields the relative contributions of these carbon sources:

$$\%^{13}C_{TCC}[TCC]=\%^{13}C_{Inoc-C}[Inoc]+\%^{13}C_{Ac-C}E_{Ac}[Ac]+\%^{13}C_{Fe-C}R_{C/Fe}[Fe(II)]+\%^{13}C_{NTA-C}[NTA]$$

Where *[Inoc], [Ac], [Fe(II)]* and *[NTA]* are the concentrations of the different carbon pools (initial inoculum, acetate assimilation, carbon fixation through Fe(II) oxidation, and acquisition of carbon from Fe(III)-NTA breakdown) contributing to total cell carbon *[TCC]*. E_{Ac} denotes the net efficiency of acetate assimilation, $R_{C/Fe}$ the net ratio of molecules of CO_2 fixed into cell carbon per atoms of Fe(II) oxidized. $\%^{13}C_{Inoc\text{-}C}$, $\%^{13}C_{Ac\text{-}C}$, $\%^{13}C_{Fe\text{-}C}$ and $\%^{13}C_{NTA\text{-}C}$ indicate the isotopic composition of cell carbon derived from these different sources, respectively. $\%^{13}C_{TCC}$ is the isotopic composition of total cell carbon, as measured in the isotope labeling experiments in this study (Table 1).

The net efficiency of carbon assimilation from acetate during photoheterotrophic growth of *R. capsulatus* was 1.75±0.14 mol cell C / mol acetate (E_{Ac} =88% carbon conservation efficiency, average from 5 biological replicates ± SD), in agreement with similar measurements for the anoxygenic phototroph *R. palustris* (Mckinlay and Harwood, 2010). The net ratio of CO_2 fixation to Fe(II) oxidation was estimated to be $R_{C/Fe}$ =0.23 since 4.3 electrons from Fe(II) are required to reduce inorganic carbon to the carbon redox state of of

R. Capsulatus biomass (-0.3, see Supporting Information for details). The contribution from the inoculum to final biomass was estimated to be 1% of the biomass generated from growth on acetate (the 1% inoculum). Assuming that acetate metabolism proceeds by very similar pathways irrespective of the presence or absence of Fe(II)-NTA metabolism and vice-versa, the mass balance equations for the different experimental conditions [A, B and C] provide the estimates for the unknown parameters ($\%^{13}C_{NTA\text{-}C}$ and *[NTA]*) reported in Table 2.

NTA breakdown products are metabolized with an exchange of ∼18.6% of assimilated carbon with the inorganic pool (either by dear boxylation/recarboxylation reactions or oxidation and refixation via the Calvin cycle), which is similar to our measured value for acetate assimilation (16.9%). The total amount of cell carbon derived from the assimilation of NTA breakdown products (0.70 mM C), corresponds to 0.12mM NTA (a 6C compound) - or 1.2% of the total NTA pool - if all carbon in the photolytic breakdown products can be metabolized by the organism. The precise rate of photolytic breakdown is difficult to estimate because Fe(III)-NTA photolysis is strongly pH and wavelength dependent, but would be expected to be slow at circumneutral (or higher) pH with little irradiation in the UV (shorter than ∼365nm) (Andrianirinaharivelo et al., 1993).

The estimate for *[NTA]* also enables calculation of an electron mass balance based on the total electron content of the generated *R. capsulatus* biomass and the total electron content of the consumed substrates (acetate, Fe(II) and NTA breakdown products). For this calculation, we assume that the oxidation state of carbon in the assimilated NTA breakdown product corresponds to the oxidation state of carbon in formaldehyde; making this assumption, we can estimate the total electron recovery for each experimental condition (Table 2).

2.4 Obligate mixotrophy

Interestingly, the model results and Figure 1 suggest that *R. capsulatus* cannot fully benefit from the assimilation of NTA breakdown products in the absence of Fe(II). In the presence of Fe(II), NTA breakdown products contribute as much as 41% to cell carbon. If provided with Fe(III)-NTA, however, this contribution is not visible in the growth curve. Because all organic carbon sources available to *R. capsulatus* in our experiments are slightly more oxidized than bulk biomass (see Supporting Information for details), the organism requires some reducing power for net biosynthetic reduction of the substrate. In the case of photoheterotrophic growth on acetate alone, the oxidation of some acetate can provide the necessary reducing power to assimilate the remaining acetate, ultimately contributing to the observed suboptimal efficiency (88%) of acetate assimilation. In the case of NTA breakdown products, however, some of the reducing power available from the oxidation of Fe(II) might be required to fully benefit from these carbon sources (hypothesized pathway, Figure 2). If this were the case, the observed phototrophic growth on Fe(II)-NTA would be truly obligate photomixotrophy. This possibility cannot be fully resolved here but provides a testable hypothesis for further research. Detailed metabolic flux experiments could help elucidate the interdependence of these pathways and explore the role Fe(II) oxidation might play in the assimilation of refractory organic carbon sources. Analogously, the ambiguous function of Fe(II) oxidation in anaerobic chemotrophic Fe(II) oxidizers (Kappler et al.,

2005) might similarly be explained by considering Fe(II) oxidation as an auxiliary mechanism for redox balancing during the assimilation of organic carbon.

3. Conclusion

The existence of mixotrophic growth itself is not surprising and has previously been suggested to occur both in phototrophic (Widdel et al., 1993) and chemotrophic (Hallbeck and Pedersen, 1991)Fe(II) metabolisms. However, its significance is rarely appreciated despite its likely importance in nature. Our results show that an organism not previously considered capable of growing by Fe(II) oxidation, in fact originally thought *incapable* of oxidizing Fe(II) altogether, can use Fe(II) for growth under certain conditions. The ability to grow photomixotrophically on Fe(II) might be more widespread than previously assumed, even for cultured organisms that have simply not been exposed to conditions that allow this mode of growth to be observed in the laboratory. It will be interesting to learn whether mixotrophic growth accounts for a significant proportion of cellular Fe(II) oxidation activity by different types of Fe(II) oxidizing organisms. Future research into the different enzymatic pathways of Fe(II) oxidation and a more detailed understanding of their regulation could permit a more accurate assessment of how widespread and environmentally significant microbial Fe(II) oxidation is today and has been throughout Earth's history.

4. Materials and Methods

4.1 Experimental conditions

Rhodobacter capsulatus SB1003 was grown phototrophically in anoxic, minimal-salts freshwater medium, prepared as previously described (Ehrenreich and Widdel, 1994). The medium was buffered at pH 7.0 with 22mM sodium bicarbonate. All experiments were prepared in an oxygen- and hydrogen-free, anaerobic chamber under an atmosphere of pure N_2. All reagents and glassware were stored in the chamber at least three days prior to use to remove traces of oxygen. In addition to standard heat sterilization procedures used for all equipment and medium preparation, glassware was precombusted in a muffle furnace at 550°C to remove all remaining traces of organic materials potentially adhered to the glass. Cells were grown an aerobically at 30°C under constant illumination from two 60W incandescent light sources at 30cm distance, providing a total irradiance of ca. 40 W/m^2 (45.5% visible light, 54.4% IR, ∼0.1% UV). Growth was followed by optical density at 675nm (OD675). This wavelength was used to decrease distortion by Fe(III)-NTA, which absorbs strongly at 600nm. OD675 underestimates optical density as compared to a measurement at 600nm.

4.2 Phototrophic growth in the presence of iron

Phototrophic growth was assessed in bicarbonate buffered freshwater medium amended with 4mM ferrous Fe(II) complexed by 10mM nitrilotriacetate (NTA), or 5mM ferric Fe(III) complexed by 10mM NTA. Medium amended with either 5mM NTA only or with Fe(II)-NTA incubated in the dark was tested as controls. No additional carbon or electron sources were provided. NTA was chosen as the complexing agent to avoid fast photolytic breakdown of the Fe(III)-ligand complex. Previous work with citrate revealed a high degradation of the more photoreactive Fe(III)-citrate complex (∼0.6 mM / day, Caiazza et

al., 2007)), which allowedrapid accumulation of acetoacetate, a substrate that can be readily metabolized by *R. capsulatus* and obscures the effect of Fe(II) oxidation. The chosen concentrations of NTA were previously found not to interfere with growth on other substrates (data not shown) while ensuring virtually all Fe(II) and Fe(III) remain complexed, preventing precipitation of iron hydroxides (Poulain and Newman, 2009). Experiments were conducted in biological triplicates. Fe(II) concentrations were measured at the start and end of the experiment. Fe(II) was quantified throughout this study using the FerroZine assay (Stookey, 1970).

4.3 Isotope labeling

For isotope labeling, freshwater medium was buffered with 22mM labeled sodium bicarbonate ($NaH^{13}CO_3$, CAS# 87081-58-01) purchased from Cambridge Isotope Laboratories, Inc. (catalogue # CLM-441, purification grade: >99% ^{13}C). Freshwater medium was amended with 3mM acetate only [A], ∼4mM Fe(II)-10mM NTA only [B], or both [C]. Cultures were harvested upon reaching early stationary phase (20 hours after inoculation for [A], 29 hours for [B, C]), washed thrice in deionized water and lyophilized overnight. Acetate and Fe(II) concentrations were determined before inoculation and at the time of harvest. Acetate was measured using a Dionex ICS-3000 ion chromatography system with a 4×240mm AS-11 IonPac column and NaOH elution gradient (0.5 to 5.0 mM NaOH in 3.5 min followed by 5.0 to 37mM NaOH in 12 min at a flow rate of 2 ml/min). Isotopic composition of bulk cell carbon was determined by EA-IRMS at the UC Davis Stable Isotope Facility (Davis, CA). Carbon isotopic compositions from labeled experiments are reported in terms of atom percent $\%^{13}C = 100\ [^{13}C / (^{12}C + {}^{13}C)]$ throughout this study. Isotopic composition of acetate, NTA as well as the in oculum culture used in this study were measured and confirmed to be approximately natural abundance ($\approx$ 1.1 $\%^{13}C$, $\delta^{13}C$ > 40‰, data not shown). The labeled bicarbonate was assumed to comply with the manufacturer's specifications ($\approx$ 99 $\%^{13}C$). Experiments were conducted in biological triplicates [A] or quadruplicates [B, C]. Abiotic controls indicated no significant oxidation of Fe(II) over the course of the experiment.

4.4Carbon assimilation efficiency

The carbon assimilation efficiency of *R. capsulatus* during phototrophic growth on acetate was determined from the consumption of acetate and concomitant increase in cell dry weight of cultures grown to late exponential phase on acetate as the only carbon source. Cultures were pelleted by centrifugation, filtered onto pre-weighed Spin-X centrifuge tube filters and dried to constant weight in a 60°C drying oven. Total cell carbon content was derived from dry weights based on the elemental composition of *R. capsulatus* ($CH_{1.83}N_{0.183}O_{0.5}$, Dorffler et al., 1998). Acetate consumption was measured by ion chromatography.

Supplementary Material

Refer to Web version on PubMed Central for supplementary material.

Acknowledgments

We thank Alexandre Poulain for teaching S.K. how to work with *R. capsulatus* and Alexa Price-Whelan and other members of the Newman Lab for stimulating discussions. Three anonymous reviewers are gratefully acknowledged for constructive criticism. This work was supported by grants to D.K.N. from the National Science Foundation (grant MCB-0616323) and the Howard Hughes Medical Institute. D.K.N. is an Investigator of the Howard Hughes Medical Institute.

References

Andrianirinaharivelo SL, Pilichowski JF, Bolte M. Nitrilotriacetic acid transformation photo-induced by complexation with iron(III) in aqueous solution. Transition Metal Chemistry. 1993; 18:37–41.

Bauer C, Elsen S, Swem L, Swem D, Masuda S. Redox and light regulation of gene expression in photosynthetic prokaryotes. Philos T Roy Soc B. 2003; 358:147–153.

Blasco R, Cardenas J, Castillo F. Acetate metabolism in purple non-sulfur bacteria. FEMS Microbiology Letters. 1989; 58:129–132.

Bunescu A, Besse-Hoggan P, Sancelme M, Mailhot G, Delort AM. Fate of the nitrilotriacetic Acid-Fe(III) complex during photodegradation and biodegradation by *Rhodococcus rhodochrous*. Applied and Environmental Microbiology. 2008; 74:6320–6326. [PubMed: 18757580]

Caiazza NC, Lies DP, Newman DK. Phototrophic Fe(II) Oxidation Promotes Organic Carbon Acquisition by *Rhodobacter capsulatus* SB1003. Applied and Environmental Microbiology. 2007; 73:6150–6158. [PubMed: 17693559]

Chistoserdova L, Chen S, Lapidus A, Lidstrom M. Methylotrophy in *Methylobacterium extorquens* AM1 from a genomic point of view. Journal of Bacteriology. 2003; 185:2980–2987. [PubMed: 12730156]

Croal LR, Jiao Y, Newman DK. The fox operon from *Rhodobacter* strain SW2 promotes phototrophic fe(II) oxidation in *Rhodobacter capsulatus* SB1003. Journal of Bacteriology. 2007; 189:1774–1782. [PubMed: 17189371]

Dobbin P, Warren L, Cook N, McEwan A, Powell A, Richardson D. Dissimilatory iron(III) reduction by *Rhodobacter capsulatus*. Microbiol-Uk. 1996; 142:765–774.

Dorffler M, Steindorf A, Oelze J. Determination of C/N ratios required for de-repression of nitrogenase in *Rhodobacter capsulatus*. Z Naturforsch C. 1998; 53:961–967.

Ehrenreich A, Widdel F. Anaerobic Oxidation of Ferrous Iron by Purple Bacteria, a New-Type of Phototrophic Metabolism. Applied and Environmental Microbiology. 1994; 60:4517–4526. [PubMed: 7811087]

Ehrlich HL, Newman DK. Geomicrobiology. 2008:279.606.

Filatova L, Berg I, Krasil'nikova E, Tsygankov A, Laurinavichene T, Ivanovsky R. A study of the mechanism of acetate assimilation in purple nonsulfur bacteria lacking the glyoxylate shunt: Acetate assimilation in *Rhodobacter sphaeroides*. Microbiology+. 2005; 74:265–269.

Hallbeck L, Pedersen K. Autotrophic and mixotrophic growth of *Gallionella ferruginea*. Journal of General MIcrobiology. 1991; 137:2657–2661.

Hillmer P, Gest H. H2 metabolism in the photosynthetic bacterium *Rhodopseudomonas capsulata*: H2 production by growing cultures. Journal of Bacteriology. 1977; 129:724–731. [PubMed: 838685]

Kappler A, Straub K. Geomicrobiological cycling of iron. Rev Mineral Geochem. 2005; 59:85–108.

Kappler A, Schink B, Newman DK. Fe(III) mineral formation and cell encrustation by the nitrate-dependent Fe(II)-oxidizer strain BoFeN1. Geobiology. 2005; 3:235–245.

Larson RA, Stabler PP. Sensitized photooxidation of nitrilotriacetic and iminodiacetic acids. Journal of Environmental Science and Health Part A: Environmental Science and Engineering. 1978; 13:545–552.

Mckinlay JB, Harwood CS. Inaugural Article: Carbon dioxide fixation as a central redox cofactor recycling mechanism in bacteria. Proceedings of the National Academy of Sciences. 2010; 107:11669–11675.

Mckinlay JB, Harwood CS. Calvin Cycle Flux, Pathway Constraints, and Substrate Oxidation State Together Determine the H2 Biofuel Yield in Photoheterotrophic Bacteria. mBio. 2011; 2:e00323-00310–e00323-00310. [PubMed: 21427286]

Meister M, Saum S, Alber B, Fuchs G. L-malyl-coenzyme A/beta-methylmalyl-coenzyme A lyase is involved in acetate assimilation of the isocitrate lyase-negative bacterium *Rhodobacter capsulatus*. Journal of Bacteriology. 2005; 187:1415–1425. [PubMed: 15687206]

Poulain AJ, Newman DK. Rhodobacter capsulatus Catalyzes Light-Dependent Fe(II) Oxidation under Anaerobic Conditions as a Potential Detoxification Mechanism. Applied and Environmental Microbiology. 2009; 75:6639–6646. [PubMed: 19717624]

Richardson DJ, King GF, Kelly DJ, McEwan AG, Ferguson SJ, Jackson JB. The role of auxiliary oxidants in maintaining redox balance during phototrophic growth of *Rhodobacter capsulatus* on propionate or butyrate. Arch Microbiol. 1988; 150:131–137.

Stolzberg RJ, Hume DN. Rapid formation of iminodiacetate from photochemical degradation of iron (III) nitrilotriacetate solutions. Environ Sci Technol. 1975; 9:654–656.

Stookey LL. Ferrozine - a new spectrophotometric reagent for iron. Analytical Chemistry. 1970; 42:779–781.

Tabita F. Research on carbon dioxide fixation in photosynthetic microorganisms (1971-present). Photosynth Res. 2004; 80:315–332. [PubMed: 16328829]

Tichi M, Tabita F. Maintenance and control of redox poise in Rhodobacter capsulatus strains deficient in the Calvin-Benson-Bassham pathway. Arch Microbiol. 2000; 174:322–333. [PubMed: 11131022]

Tichi M, Tabita F. Interactive control of Rhodobacter capsulatus redox-balancing systems during phototrophic metabolism. Journal of Bacteriology. 2001; 183:6344–6354. [PubMed: 11591679]

Trott T, Henwood RW, Langford CH. Sunlight photochemistry of ferric nitrilotriacetate complexes. Environ Sci Technol. 1972; 6:367–368.

Widdel F, Schnell S, Heising S, Ehrenreich A, Assmus B, Schink B. Ferrous iron oxidation by anoxygenic phototrophic bacteria. Nature. 1993; 362:834–836.

Willison JC. Pyruvate and Acetate Metabolism in the Photosynthetic Bacterium *Rhodobacter capsulatus*. Journal of General MIcrobiology. 1998; 134:2429–2439.

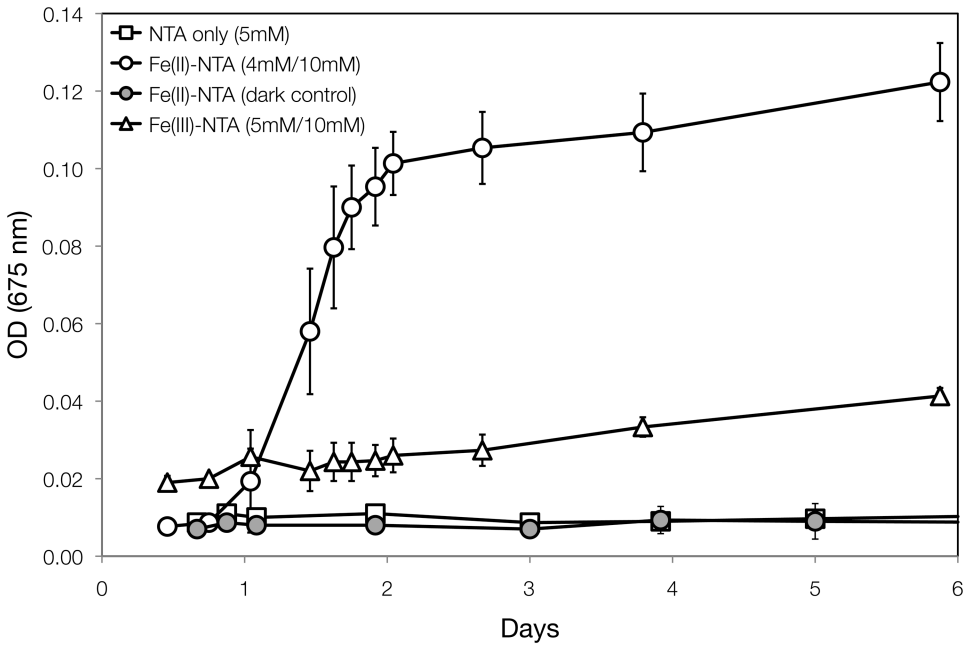

Figure 1. Fe(II) oxidation promotes growth

Phototrophic growth was assessed in freshwater medium amended with NTA only, ferrous Fe(II)-NTA (light and dark), or ferric Fe(III)-NTA. Symbols represent the averages of biological triplicates. Error bars indicate standard deviation and may be smaller than symbol size. OD (675nm) is optical density at 675nm.

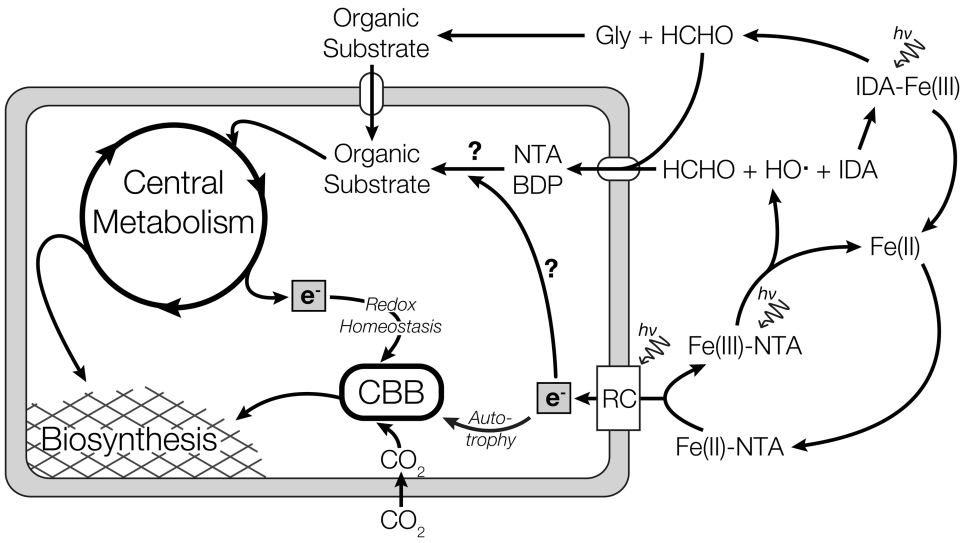

Figure 2. Mixotrophic growth of *R. capsulatus*

Schematic overview of the various pathways that can contribute to photomixotrohpic growth in the presence of Fe(II)-NTA. Question marks (?) indicate hypothesized pathways (discussed in text) that require further investigation. Abbreviations: Calvin-Benson-Bassham pathway (CBB), photosynthetic reaction center (RC), NTA breakdown products (NTA BDP), photochemically/photosynthetically active radiation (*hv*).

Table 1

Fe(II) oxidation allows carbon fixation

Bulk isotopic composition of *R. capsulatus* after phototrophic growth in freshwater medium containing 22mM $H^{13}CO_3^-$ and amended with acetate only [A], Fe(II)-NTA only [B], or both [C]. Optical density (OD at 675nm), acetate and ferrous Fe(II) concentrations were measured at inoculation (t=0) and at the time of harvest (20 hours after inoculation for [A], 29 hours for [B, C]). Values represent averages of biological triplicates [A] and quadruplicates [B, C] respectively. Reported error is one standard deviation.

Sample	OD (675nm)		Acetate [mM]		Fe(II) [mM]		Bulk ^{13}C [%]
	Inoculation	Harvest	Start	End	Start	End	
Acetate only [A]	0.007±0.001	0.353±0.001	3.02±0.03	<0.1*	none	none	16.8±0.1
Fe(II)-NTA only [B]	0.007±0.001	0.145±0.003	none	none	4.31±0.08	0.21±0.03	62.8±0.5
Acetate & Fe(II)-NTA [C]	0.008±0.003	0.451±0.026	3.02±0.03	<0.1*	4.32±0.13	0.33±0.11	28.1±0.3

*Acetate at time of harvest could no longer be detected and is reported to be below the lower limit of determination.

Table 2

Carbon and electron mass balance

Carbon mass balance includes total amounts and isotopic composition of cell carbon derived from the different carbon sources. Electron recovery is based on total e- donor consumption and cellular e- content. Derived quantities are reported with errors derived by error propagation. Reported error is one standard deviation.

Carbon sources	Derived cell carbon		Acetate only [A]	Fe-NTA only [B]	Acetate & Fe-NTA [C]
	[mM C]	[% ^{13}C]	Relative contributions [%C-source]		
Inoculum	0.05±0.01	1.1	1.0±0.2%	3.1±0.4%	0.8±0.1%
Acetate assimilation	5.3±0.4	16.9	99.0±0.2%	—	76±2%
Carbon fixation by Fe oxidation	0.95±0.07	99.0	—	56±6%	14±1%
Assimilation of NTA breakdown products	0.7±0.2	18.6	—	41±6%	10±1%
Total biomass C [mM]			5.3±0.4	1.7±0.2	7.0±0.5
Total biomass e^- [mM] *			22.9±2.4	7.3±0.9	29.9±2.9
Total e-donor e^- [mM] #			24.4±0.3	7.1±0.8	31.2±0.8
e-recovery [%] +			94±10%	103±18%	96±10%

* based on e^- content of *R. capsulatus* biomass derived in Supplemental Information

assuming substrate from NTA breakdown to be primarily in the oxidation state of formaldehyde (see Table S1)

+ ratio of total e^- recovered in biomass / e^- available from e-donors